frontiers in Marine Science

ORIGINAL RESEARCH
published: 24 July 2020
doi: 10.3389/fmars.2020.00613

Response to Sea Ice Melt Indicates High Seeding Potential of the Ice Diatom *Thalassiosira* to Spring Phytoplankton Blooms: A Laboratory Study on an Ice Algal Community From the Sea of Okhotsk

Dong Yan[1], Kazuhiro Yoshida[2], Jun Nishioka[3], Masato Ito[4,5], Takenobu Toyota[4] and Koji Suzuki[1,2]**

[1] Graduate School of Environmental Science, Hokkaido University, Sapporo, Japan, [2] Faculty of Environmental Earth Science, Hokkaido University, Sapporo, Japan, [3] Pan–Okhotsk Research Center, Institute for Low Temperature Science, Hokkaido University, Sapporo, Japan, [4] Institute of Low Temperature Science, Hokkaido University, Sapporo, Japan, [5] Institute of Arctic Climate Environment Research, Japan Agency for Marine-Earth Science and Technology, Yokosuka, Japan

OPEN ACCESS

Edited by:
Susana Agusti,
King Abdullah University of Science and Technology, Saudi Arabia

Reviewed by:
Maria Vernet,
University of California, San Diego, United States
Kalle Olli,
University of Tartu, Estonia

***Correspondence:**
Dong Yan
yan@ees.hokudai.ac.jp
Koji Suzuki
kojis@ees.hokudai.ac.jp

Specialty section:
This article was submitted to Aquatic Microbiology, a section of the journal Frontiers in Marine Science

Received: 17 April 2020
Accepted: 06 July 2020
Published: 24 July 2020

Citation:
Yan D, Yoshida K, Nishioka J, Ito M, Toyota T and Suzuki K (2020) Response to Sea Ice Melt Indicates High Seeding Potential of the Ice Diatom Thalassiosira to Spring Phytoplankton Blooms: A Laboratory Study on an Ice Algal Community From the Sea of Okhotsk. Front. Mar. Sci. 7:613. doi: 10.3389/fmars.2020.00613

Phytoplankton communities in seasonally ice-covered areas are largely affected by ice algae. The Okhotsk Sea is the southernmost sea ice zone in the northern hemisphere with a sizeable seasonal ice cover, thus ice algae of the Okhotsk sea ice have a large potential to seed the early spring bloom. Little is known about the Okhotsk ice algal communities and their seeding effects. We investigated the dynamics of the composition and the photophysiological performances of an Okhotsk ice algal community in a 6-day laboratory incubation experiment that simulated the natural ice melt conditions. Centric diatoms, especially *Thalassiosira* spp., overwhelmingly dominated the ice algal community throughout incubation, whereas pennate diatoms, mostly *Navicula* and *Nitzschia*, showed little growth with much higher mortality. The maximum photochemical efficiency of Photosystem II (F_v/F_m) was the lowest at the beginning of the ice melt, suggesting a suppressed photosynthetic functioning by changes in salinity. The cellular pigment contents decreased by 30% due to osmotic stress, evidenced by deformed plastids under a microscope. The transcript level of the *rbcL* gene that encodes the large subunit of RubisCO was significantly higher during ice melt and decreased in the no-ice period, suggesting an urgent need for carbon fixation under the melt condition. Full recovery of photosynthesis and growth was also made after complete ice melt. Our results indicated high seeding potential of *Thalassiosira* to spring blooms owing to their photophysiological plasticity to dynamic salinity changes.

Keywords: ice algae, diatom bloom, *Thalassiosira*, osmotic stress, photophysiology, seeding effect, Sea of Okhotsk

INTRODUCTION

Sea ice algae can form a large fraction of sea-ice biomass (Tedesco et al., 2019). Previous studies suggested that the release of ice algae into the water column initiated the spring development of phytoplankton (Garrison et al., 1987; Garrison and Close, 1993), which is known as the seeding effect of ice algae. There is a substantial standing stock of ice algae in the Okhotsk Sea ice. Dense

ice algal communities have commonly been observed at the bottom of Okhotsk sea ice, especially in spring (Leonov et al., 2007). Chlorophyll *a* (Chl *a*) concentrations in the Okhotsk sea ice ranged between 0.2 to 3.5 mg m^{-2}, and was up to an order of magnitude higher than the under-ice seawater (Granskog et al., 2015). McMinn et al. (2008) reported an extremely high Chl *a* concentration of 1.6×10^3 mg Chl *a* m^{-3} in the pack ice near Shiretoko with an average thickness of around 70 cm. Granskog et al. (2015) also found considerable excess protein-like compounds in the Okhotsk Sea ice relative to the under-ice seawater, suggesting active biological production within the ice.

The annual primary production in the Sea of Okhotsk is largely derived from spring diatom blooms following the sea ice melt (Ohwada, 1956; Zhang et al., 2006). The spring blooms usually continue until the end of June in the central areas and mid-July or early August in the colder eastern and northern parts (Sorokin and Sorokin, 1999; Shuntov, 2001). When ice breakup begins in spring, ice algae are rapidly washed out of the ice and dispersed into the water column, causing a significant increase in the downward flux of ice algal cells under the Okhotsk sea ice (Leonov et al., 2007; Hiwatari et al., 2008). Spring phytoplankton communities in coastal southern Okhotsk waters off Hokkaido, Japan can also be directly affected by ice melting. High Chl *a* concentrations of around 30 and 60 mg m^{-3} have been observed in the southern part of the Sea of Okhotsk and the coastal waters of Mombetsu Harbor during the ice melt season (Taguchi et al., 2000; Kanna et al., 2018). Such high Chl *a* concentration could be attributed to the released ice algal cells. Longer periods of ice cover corresponded to larger magnitudes of the spring Chl *a* peak of the ice edge blooms in the Southern Okhotsk because this condition would favor algal growth and accumulation at the surface water (Kudoh, 1993; Mustapha and Saitoh, 2008). Besides, there are possibilities that the Okhotsk sea ice algae also contribute to the phytoplankton growth in the Oyashio waters of the western North Pacific. Pack ice often flows out into the North Pacific through the southern passes of the Kuril Islands, indicating the pack ice could be one of the sources of the highly productive coastal Oyashio waters and influences ocean conditions off the southeast coast of Hokkaido, Japan (Ohtani, 1989; Talley and Nagata, 1995). It is thus likely that ice algae in the Okhotsk sea ice have a seeding effect on the spring phytoplankton bloom of subarctic waters near Japan (Kuroda et al., 2019).

Not all of the algal cells would remain active after leaving the sea ice habitat. The released ice algae may either continue to grow in seawater to become the seed of the phytoplankton bloom after ice retreat or disappear from the water column over time (Haecky et al., 1998; Mundy et al., 2011; Kauko et al., 2018). Their disappearance would be results of fast cell sedimentation (Michel et al., 1997; Haecky et al., 1998), cell death caused by predation, or necrosis due to rapid environmental changes as ice melts (Grant and Horner, 1976; Taguchi et al., 1997; Różańska et al., 2009; Rajanahally et al., 2014). Ice algae live in brine of sea ice. The brine salinity is determined by the ice temperature (Assur, 1960; Horner, 1985). At extreme temperatures in winter, brine salinity can be 6–7 times higher than that of typical seawater at the upper part of the sea ice (Ewert and Deming, 2013). Brine salinity would be milder at the bottom part of the sea ice but can still reach 50 in the dense brownish algal layer (Grant and Horner, 1976). During the ice melt season, the brine in sea ice is generally washed out by the nearly fresh surface meltwater (Zhang et al., 1999; Notz and Worster, 2009). Ice algae thus can experience significant changes in salinity when ice melts. The ice temperature usually ranges from −4.5 to −1.8°C from the upper to the bottom part in the southern Sea of Okhotsk (Toyota et al., 2007), which corresponds to brine salinities ranging from around 75 to 32 (Assur, 1960; Horner, 1985). The average salinity of the surface seawater in this region is around 32.4 in winter. While the salinity drops to values <29 if there is a layer of melted sea ice in surface waters (unpublished data).

Salinity change during ice melt could cause drastic changes in the physiology of ice algae as they are flushing out of sea ice (Arrigo and Sullivan, 1992; Taguchi et al., 1997; Ralph et al., 2007; Ryan et al., 2011). Laboratory experiments found that ice diatoms are capable of maintaining a relatively high growth rate within a wide range of salinity of 10 to 50 (Smayda, 1969; Grant and Horner, 1976; Baars, 1982). In the most extreme case, some ice diatoms were able to grow exponentially in brine with a salinity of 105 at −6°C (Aletsee and Jahnke, 1992). However, there was usually a lag period before normal growth can be reached after being exposed to extreme salinities. The lag period, which varies among species, could occur when ice algal cells rearrange the metabolism to protect themselves from the acute osmotic shock. In other words, algal cells may die of osmotic stress before they can acclimate to the new salinity. Salinity changes severely disturb the cellular homeostasis caused by differences between the internal and exogenous concentration of inorganic ions (Guillard and Ryther, 1962). This could lead to photosynthesis and growth inhibition, respiration increase, and cell deformation in diatoms (Qasim et al., 1972; Jahnke and Baumann, 1983; Rijstenbil et al., 1989; Yoshida et al., 2020). Indirect damages mediated by the liberation of reactive oxygen species also causes additional oxidative stress (Hernando et al., 2015). Krell et al. (2007) demonstrated that the dominant ice organisms need to be well adapted or acclimated to a dynamic salinity regime coping with both hypersaline stress during ice formation and hyposaline stress during ice melt. Physiological acclimation of released ice algae is thus needed in order to grow and survive in the seawater.

The Sea of Okhotsk is a marginal sea of the subarctic North Pacific and is the southernmost sea in the northern hemisphere with a sizeable seasonal sea ice cover (Ohshima et al., 2005). Sea ice is primarily produced on the northwestern shelf of the Sea of Okhotsk and off East Sakhalin, and then advected southward due to the transportation of the prevailing northwesterly winds and the East Sakhalin Current (Martin et al., 1998; Fukamachi et al., 2009). The formation of the dense shelf water and the Okhotsk Sea intermediate water, which become a source water for the North Pacific Intermediate Water, is also driven by this wintertime brine rejection associated with the ice formation (Shcherbina et al., 2003). Sea ice develops southward, reaches a maximum in February or March by covering 50–90% of the sea, and melts away in late May or early June (Ohshima et al., 2006). According to Japan Meteorological Agency (2020), the maximum sea ice extent in the Sea of Okhotsk from 1971 to 2019 has declined by 0.062×10^6 km^2 per decade,

corresponding to a loss of 3.9% of the total sea area per decade. Despite the large biomass of the Okhotsk ice algae, the ecology and their seeding roles toward the spring blooms are not fully understood. We conducted a laboratory experiment simulating the field ice melt and measured the changes in the community composition during and after complete ice melt. We investigated the ice diatom composition of the Okhotsk sea ice using both light microscopy and the high-throughput sequencing method in order to get a more complete picture of the community. Since the survival and growth is directly related to the photosynthesis of algal cells, we also measured algal photosynthesis in the seawater, including the maximum photochemical quantum efficiency of Photosystem II (PSII, F_v/F_m), pigment composition, and the transcript levels of *rbcL* gene. The *rbcL* gene encodes the large subunit of the Ribulose-1,5-bisphosphate carboxylase/oxygenase (RubisCO) and was used as an indicator of carboxylation activity. We hypothesize that fast photophysiological acclimation to changing salinities provides competitive advantage during ice melt.

MATERIALS AND METHODS

Experimental Set-Up

A sea ice core was collected from the southeastern part of the Sea of Okhotsk (44.83°N, 144.52°E) aboard the icebreaker Patrol Vessel *Soya* (Japan Coast Guard) on February 9, 2019. During the sea ice expedition, the day time air temperature was around −8°C. The average surface seawater temperature was around −1.84°C. The ice core used was 27 cm in length and 14 cm in diameter. The sea ice temperature ranged from −4.7°C at the surface to −1.90°C at the bottom. The sampled ice core was immediately covered with semi-transparent polyethylene bags and stored in a −5°C freezer in the dark for 3 weeks until further analysis. The temperature of −5°C was used for two reasons. The first reason is according to the phase equations of sea ice, the threshold for fluid permeability in sea ice occurs at a temperature of about −5°C for sea ice with a bulk salinity of 5 (Ewert and Deming, 2013). Lower temperatures may cause much more cell death due to the long-time transportation of the ice samples to our laboratory on land. The other reason is −5°C was similar to the ice temperature at the top part of the sea ice measured in the field (i.e., −4.7°C). Ice algal cells were thus expected to survive at such a temperature. They were stored in darkness to minimize changes in the community composition.

For the melt experiment, the bottom 5 cm of the ice core with dense yellow–brown color was cut off with a stainless saw in dim light. Then the bottom was further equally divided into four pieces of around 200 g. Each piece of ice was kept in an acid-cleaned 2 L glass beaker filled with 200 mL Okhotsk seawater with a salinity of 32.2 in a freezer incubator for 2 days for recovery and acclimation to the incubation environment. The volume of sea ice and seawater used was calculated to mimic the salinity changes in the field (from 32.4 to around 29). The beakers and the seawater were autoclaved at 121°C for 20 min before use. The seawater used in this study was filtered through Whatman GF/F glass fiber filters (nominal pore size 0.7 μm, Whatman, United Kingdom) before sterilization. During the acclamation of 2 days, the freezer was set at −3°C to minimize ice growth and ice melt. The light was provided by a white LED light source (LMGA1WG21K50A4-10F, Prince Industry Inc., Japan) specially designed for freezing environments placed at the upper part of the incubator. The irradiance level was measured by a 4 π sensor (QSL-2101, Biospherical Instruments Inc., United States). In the field, the irradiance levels beneath sea ice at the beginning of the sea ice melt would not be high due to the presence of the snow and ice cover. Thus, 50 μmol photons m^{-2} s^{-1} was used for incubation. During the acclimation of 2 days, F_v/F_m increased from 0.28 to 0.56, indicating 2 days was enough for the acclimation. After the acclimation, 1.5 L sterilized *in situ* seawater was added to each 2 L beaker with the ice piece, and the temperature was adjusted to around 0°C to simulate the ice melt condition (Taguchi et al., 2000; Hiwatari et al., 2008). Water samples were taken at the time of 0, 1, 2.5, 10, 24, 31, 55, 79, 103, and 127 h, hereafter t_0, t_1, $t_{2.5}$, t_{10}, t_{24}, t_{31}, t_{55}, t_{79}, t_{103}, and t_{127}, respectively. During the melting process, the water temperature was monitored using a digital thermometer with its sensor soaked in one of the beakers. Water temperature and salinity were measured and recorded before each sampling using a digital salinometer with a conductivity temperature sensor (TetraCon® 325, Wissenschaftlich-Technische Werkstätten GmbH, Germany) (**Supplementary Figure S1**). Cell suspensions in beakers were stirred three times a day using a stainless rod to prevent settling. Because almost all of the ice has completely melted out after an incubation of 31 h, the whole incubation was divided into two parts: the ice melt period and the no-ice period by t_{31}.

Light Microscopy

To avoid a rapid change of salinity in the beakers caused by ice melt, there was a limitation on the volume of water that can be taken during each sampling. Each time we took around 25 mL water from the beaker before ice was completely melted. This resulted in a final water salinity of around 29 at the end of the incubation. A small fraction of around 5 g from the ice core bottom was also sampled and melted with 20 mL seawater for species identification. These water samples were stored in the dark at 4°C before analysis under an inverted light microscope (CKX41-FI, Olympus, Japan). Diatoms in the water samples were identified and counted within a few days after each sampling. Taxonomic identification followed Tomas (1997). Identifications were to the species level if possible but to the genus in most cases. To calculate the growth rate, cell abundance was natural log transformed before plotting against the day of incubation and the specific growth rate (μ, day^{-1}) was calculated as the slope of the linearly fitted curve.

Cell Viability

To distinguish between live and dead cells, cells in water samples of 5 mL were stained with the LIVE/DEAD™ *Bac*Light™ stain (Thermo Fisher Scientific, Inc., United States) for 30 min in the dark. Then the sample was filtered onto black 25 mm polycarbonate membrane filters (0.2 μm in pore size, Whatman Nuclepore™, United Kingdom) and stored at −80°C

until analysis with an epifluorescence microscope (BZ-9000, KEYENCE, Japan) following Agusti et al. (2015).

Pigments

Samples of 5 or 10 mL were filtered onto GF/F glass fiber filters (25 mm in diameter, nominal pore size 0.7 μm, Whatman, United Kingdom) under gentle vacuum pressure (<0.013 MPa). The filter samples were immediately frozen in a deep freezer at −80°C for later analysis. Pigment extraction and analysis were conducted according to Suzuki et al. (2015) using the *N*,*N*-dimethylformamide (DMF) bead-beating technique and Ultra-High Performance Liquid Chromatography (UHPLC). The identified pigments were grouped into photosynthetic carotenoids [PSC = fucoxanthin (Fxn)], photoprotective carotenoids [PPC = diadinoxanthin + diatoxanthin + β− carotene (Car)] and total chlorophyll (TChl = Chl *c* + Chl *a*) (Roy et al., 2011).

qPCR and RT-qPCR of *rbcL*

For the DNA and RNA analysis, water samples were filtered onto polycarbonate nucleopore filters (pore size 2 μm, Whatman, United Kingdom) with gentle vacuum pressure (0.013 M**P**a). Then the filters were stored in a deep freezer at −80°C until extraction. DNA and RNA extraction and the qPCR and RT-qPCR of the *rbcL* gene were conducted following Endo et al. (2013) and Endo et al. (2015), respectively.

Metabarcoding of Diatom-Derived 18S rRNA Gene

The diatom-derived 18S rRNA gene (rDNA) including the V4 region was amplified and sequenced using the Ion Torrent sequencing technique following Endo et al. (2018). The target 18S fragment of the extracted DNA was amplified using the *TaKaRa Ex Taq*™ Hot Start Version (TaKaRa). Each DNA sample was amplified in triplicates. The amplicon was checked by 1.2% agarose gel electrophoresis, purified using AMPure XP magnetic beads (Beckman Coulter) and quantified with an Agilent 2100 Bioanalyzer using a high sensitivity DNA Kit (Agilent Technologies). The PCR templates were then diluted to a final concentration of 13 pM and mixed for the emulsion PCR using the Ion OneTouch™ 2 system with the Hi-Q™ OT2 Kit (Thermo Fisher Scientific). The products of emulsion PCR were enriched using an Ion OneTouch™ ES (Thermo Fisher Scientific) and then loaded onto an Ion 318™ v2 chip. Sequencing of the amplicon libraries was performed using an Ion Torrent PGM system with the Ion PGM™ Hi-Q™ sequencing kit (Thermo Fisher Scientific).

Signal processing, base calling, and quality filtering were conducted using the Torrent Suite™ (Thermo Fisher Scientific). Sequences with polyclonal and no match against the A-adapter were initially filtered. Further quality control was conducted using the FASTX-Toolkit[1]. The reads without the trP1 adapter or the reverse primer sequence were removed. The remaining reads that have at least 75% of bases with a quality score of 26 were kept and trimmed so that only the V4 part between 18 and 270 bp of each read was used for further analysis. Ten thousand reads for each sample were used for the taxonomic assignment. The reads were aligned and classified on the SILVAngs web interface[2] using a local nucleotide BLAST search against the non-redundant version of the SILVA SSU Ref dataset (release 132[3]). Identical reads were clustered into OTUs of >98% identity. Reads of each OTU were used for taxonomic assignments. Singletons and the taxonomic assignments other than diatoms were not used for the taxonomy analysis.

Maximum Photochemical Quantum Efficiency of Photosystem II (F_v/F_m)

The maximum photochemical quantum efficiency of Photosystem II (PSII) (F_v/F_m) was measured at each sampling time using a pulse amplitude modulated fluorometer (Water-PAM, Walz, Germany). Cell suspensions were placed in a quartz cuvette during the measurement. The saturating pulse was provided by a red-LED with a peak illumination at 620 nm and set at 4,000 μmol photons m^{-2} s^{-1} and lasted for 400 ms for all measurements (Yan et al., 2019). The maximum photochemical efficiency of PSII was calculated as $F_v/F_m = (F_m - F_o)/F_m$. F_o is the minimum fluorescence after the darkness of 30 min and F_m is the maximum fluorescence under the saturation pulse.

Statistics

Differences among different incubation time and periods were tested using one-way analysis of variance (ANOVA) and *t*-test after Levene's test for the homogeneity of variances. Multivariate analysis was conducted using the package "vegan" of R (Dixon, 2003). We used principal component analysis (PCA) to investigate the differences in community composition among different periods of incubation-the bulk ice, the ice melt period, and the no-ice period. Hellinger distance was used for the ordination. The significance of the differences among groups was tested using permutational-multivariate analysis of variance (PERMANOVA) with 999 permutations. The significance level was set at 0.05.

RESULTS

Growth Rate

The specific growth rates of the whole diatom community, the centric and pennate diatoms during the melt or no ice periods were calculated (**Figure 1**). The specific growth rate for the no-ice period from day 2 to day 6 (μ_w) showed that the community growth (0.18 ± 0.02 day^{-1}) was mainly contributed by centric diatoms (0.18 ± 0.03 day^{-1}). While the growth rate of pennate diatoms was 3.5 times slower than that of the centric diatoms during the no ice period ($p < 0.01$) and the cell abundance of pennate diatoms remained low throughout the incubation. To simplify the calculation of the algal growth during the ice melt period, we assumed that the algal cells remaining in sea ice and

[1]http://hannonlab.cshl.edu/fastx_toolkit/

[2]https://www.arb-silva.de/ngs/

[3]http://www.arb-silva.de

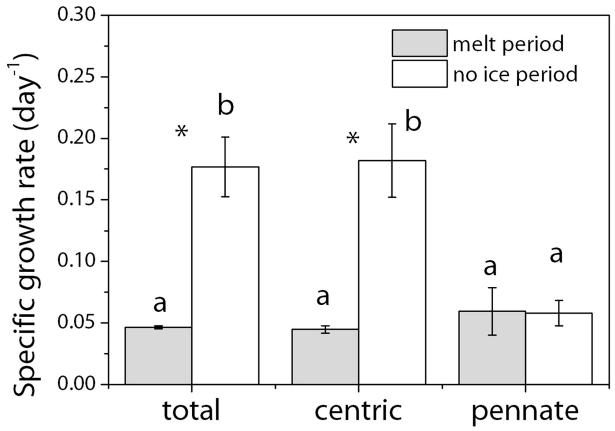

FIGURE 1 | Specific growth rate (μ, day^{-1}) of different diatom groups during the ice-melt and no-ice period. The whole incubation was divided into two parts: the ice melt period and the no-ice period by t_{31}. To calculate the growth rate in the no-ice period, cell abundance was natural log transformed before plotting against the day of incubation and the specific growth rate was calculated as the slope of the linearly fitted curve. To calculate the algal growth during the ice melt period, we assumed that the algal cells remaining in sea ice and those released into the seawater had the same growth rate. Gray, melt period; White, no-ice period. Mean values (±SD) are the average of four independent measurements. Alphabets indicate significant difference among different diatom groups. Stars indicate significant differences between the two incubation periods. ANOVA was used for comparisons. The significance level was 0.05.

those released into the seawater had the same growth rate, μ_i. By doing this we can imagine that all the algal cells were staying in sea ice until the moment ice had melted out (t_{31}) when all cells were released into the seawater. Then the total cell number at t_0 plus the increased cell number due to cell growth in sea ice would equal to the total cell number in seawater at the moment when all ice disappears.

$$N_{ice}(t_{31}) = N_{sw}(t_{31}),$$

where $N_{ice}(t_{31})$ and $N_{sw}(t_{31})$ are the cell number in sea ice and seawater at t_{31}, respectively. The total cell number in sea ice at t_{31} is

$$N_{ice}(t_{31}) = N_{ice}(t_0) \times \exp(\mu_i t_{31}). \quad (1)$$

$$N_{ice}(t_0) = c_{ice}(t_0) \times V_{ice}(t_0), \quad (2)$$

where $c_{ice}(t_0)$ is the cell concentration in the bulk ice and $V_{ice}(t_0)$ is the original volume of the sea ice used. Both of them are known. And the total cell number in seawater after all cells were released is

$$N_{sw}(t_{31}) = c_{sw}(t_{31}) \times V_{sw}(t_{31}), \quad (3)$$

where $c_{sw}(t_{31})$ is the cell concentration in the seawater and $V_{sw}(t_{31})$ is the total volume of the seawater plus the water volume used for water sampling. Both of them are known.

Then we can calculate μ_i by solving the above three equations. Results showed that despite the large difference in μ_w between centric and pennate diatoms, the calculated μ_i for the two groups were similar, around 0.05 day^{-1}, and very close to that of the μ_w of pennate diatoms in the no-ice period.

Cell Viability and Cell Structure

The percentages of dead cells in the diatom community were low (**Figure 2**). The highest percentage was around 5.89 ± 0.71% in the pennate diatoms under the ice melt condition. This percentage dropped to <2% after ice melt ($p < 0.01$). The average percentage of dead cells of centric diatoms was 0.50 ± 0.17% during ice melt and increased to 1.68 ± 0.64% in the no-ice period ($p < 0.05$).

We tracked changes in the structure of some large diatom cells with a light microscope during the incubation periods (**Supplementary Figure S2**). Most of the observed cells during ice melt looked quite different from those normal healthy-looking cells in the laboratory culture and the ones before the melting treatment. Obvious signs of salt stress include (a) loss of all or a large part of the pigments, so the chloroplasts became pale; (b) chloroplast pellets not evenly distributed or spread in a single layer close to the cell wall in the cytoplasm like that in healthy cells. Instead, chloroplast pellets formed small aggregates inside the cell; (c) visible adhesive sticky gel attached to the stressed centric diatom cells. Most of the stressed cells recovered with time during the incubation. The color of the chloroplast became brighter and darker. The mucilage around the cells became invisible. At the end of the incubation, the cells in the beakers

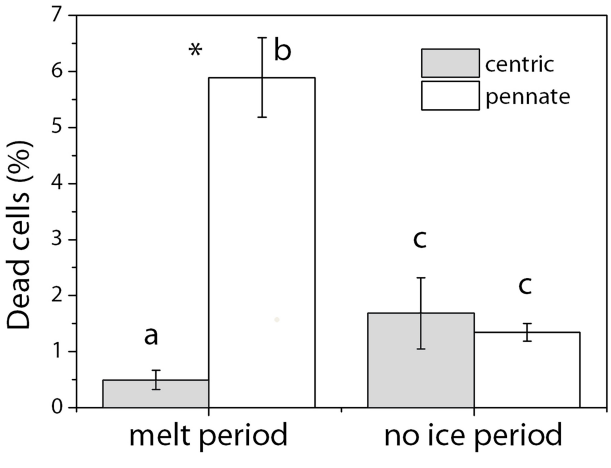

FIGURE 2 | Percentage of dead cells (%) in the diatom community during the melt period and the no-ice period. Cells in water samples were stained with the LIVE/DEAD^{TM} BacLight^{TM} stain (Thermo Fisher Scientific, Inc., United States), filtered onto black 25 mm polycarbonate membrane filters (0.2 μm in pore size, Whatman Nuclepore^{TM}, United Kingdom), and analyzed with an epifluorescence microscope (BZ-9000, KEYENCE, Japan). Gray, centric diatoms; White, pennate diatoms. Mean values (±SD) are the average of four independent measurements. Alphabets indicate significant difference among different diatom groups. Stars indicate significant differences between the two incubation periods. ANOVA was used for comparisons. The significance level was 0.05.

looked similar to the normal healthy-look cells in the laboratory culture under a microscope.

Diatom Community Composition

To make better comparisons of the results between microscopy and metabarcoding, the diatom genus or groups that shown in the figure need to meet the following two standards (**Figure 3**). (1) The top 10 abundant ones (i.e., abundance of cells or gene fragments) during the whole incubation. (2) Genus or groups that were found at each time of sampling. Other genus or groups were added up to groups of other pennates and other centrics. The complete run files of the 18S rDNA sequences have been deposited in the DDBJ Sequence Read Archive under accession number PRJDB9641. Both the light microscopy (LM) and the 18S rDNA data showed that centric diatoms dominated the communities. Genus or group contribution to the total was averaged. The top five abundant genus (groups) were *Thalassiosira* (74.7%), *Chaetoceros* (9.9%), *Porosira* (3.5%), *Nitzschia* (3.4%) and *Navicula* (2.6%) for the LM-based communities, whereas *Thalassiosira* (75.8%), *Navicula* (7.4%), *Porosira* (7.1%), the total other pennate diatoms (5.6%) and the total other centric diatoms (2.1%) for the 18S rDNA-based communities. There was an overwhelming dominance of *Thalassiosira* of >70% revealed by both methods. *Chaetoceros* was the second most abundant genus in terms of cell number, around 10%, while it was much less abundant in the 18S rDNA community (0.3%). Overall, pennate diatoms were slightly more abundant in terms of 18S rDNA sequences (14.7%) than LM cell counts (8.9%).

PCA results showed that the first component, most likely to be related to the time of incubation, explained 45.42% and 66.65% of the variance in LM and 18S rDNA metabarcoding, respectively (**Figure 4**). The biplots showed that *Thalassiosira* was more commonly found in the samples from the no-ice period for both LM and 18S communities. For the LM community, *Thalassiosira, Chaetoceros*, and *Detonula* were more related to the samples from no-ice period. Other diatoms showed various patterns in their abundance with the incubation time and were more commonly found in the ice-melt samples. For the 18S rDNA communities, *Porosira* and *Navicula* were found to be more abundant in the bulk ice than the samples that have undergone incubation. *Nitzschia* and the total other pennates were abundant at the beginning of the incubation (t_0) while decreased in number after that.

To see the changes in community composition at the species level, we constructed an 18S rDNA library for a local BLAST using the diatom isolates from the sea ice and seawater of the Sea of Okhotsk, the Saroma Lagoon adjacent to the sea, and the coastal Oyashio seawater. Species that were not successfully isolated but were abundant in the algal community in the results of LM and SILVAngs were also included in the library. In that case we used the best hit 18S rDNA sequences of the OTUs in the NGS data with 97% in similarity downloaded from the NCBI database. To make simple comparisons, the most abundant 100 OTUs in the results were used for annotation. Like the results of the PCA based on the 18S rDNA of SILVAngs database, our local BLAST also showed a significant decrease in the number of OTUs of *Navicula* and *Nitzschia* after incubation (**Supplementary Figure S3**). Despite the increase in the contribution of *Thalassiosira* to the total after incubation, the relative abundance of different *Thalassiosira* species also changed. *T. nordenskioeldii* was the most abundant one in the bulk ice, while three other *Thalassiosira* species including *T. antarctica*, *T. hyalina*, and *Thalassiosira.* sp. showed faster increases and became dominant in the community at the end.

Photophysiological Performance

The cellular pigment contents showed a decreasing trend until each minimum value was reached after 10 h of incubation (**Figure 5**), and then they increased until the end. The PSC and TChl showed similar trends that the minimum values at t_{10} were around 70% of the original ones at t_0 and the final content at t_{127} was twice than that at t_0. For the PPC, the decreasing trend was more significant than the increase. The decrease in PPC was >50% at t_{10} and the recovery, with a much slower rate than the other pigment groups, was finally completed at the end of the incubation.

The sea ice melt significantly suppressed F_v/F_m (**Figure 6**). The variation of F_v/F_m was large during the ice melt period when the cell concentrations were lower. Though being suppressed, the lowest F_v/F_m was 0.39 ± 0.05 at t_0 which means the PSII was still functional under the salt stress. F_v/F_m then increased and reached the maximum of 0.62 ± 0.01 at t_{79} and stayed at the same level until the end of the incubation.

The transcript levels of the *rbcL* gene were significantly higher during the ice melt period than that of the no-ice period (**Figure 7**). After the melt of 5 h, the gene expression began to decrease and then kept a relatively steady state until the end of the incubation. Overall, the transcript levels of the *rbcL* gene during the first 5 h were eight times higher than the average level of the steady state from t_{79} to t_{127} ($p < 0.01$).

DISCUSSION

Pennate diatoms such as *Fragilariopsis*, *Nitzschia*, and *Navicula* usually dominate sea ice algal communities (Poulin et al., 2011; Szymanski and Gradinger, 2016). While the diatom community composition of the Okhotsk Sea ice used in our study showed different patterns (**Figure 3**). Most of the abundant *Thalassiosira* found in the Okhotsk sea ice were also reported from the sea ice of the Arctic, which includes the Chukchi Sea, the East Siberian Sea, the Laptev Sea, and the Barents Sea, though their dominance was much less frequent than pennate diatoms (Hegseth, 1992; Okolodkov, 1992). The Okhotsk sea ice could be unique that the discoid chain-forming centric diatoms *Thalassiosira* often occur with high abundance (Ohwada, 1956; McMinn et al., 2008). We analyzed other sea ice samples taken during the same cruise and found that the dominance of *Thalassiosira* spp. in the Okhotsk Sea ice was not a single case (data not shown).

The dominance of *Thalassiosira* during the no-ice period in our laboratory experiment is in consistence with that in the field that the early spring bloom of *Thalassiosira* is a common phenomenon occurring in the Sea of Okhotsk and

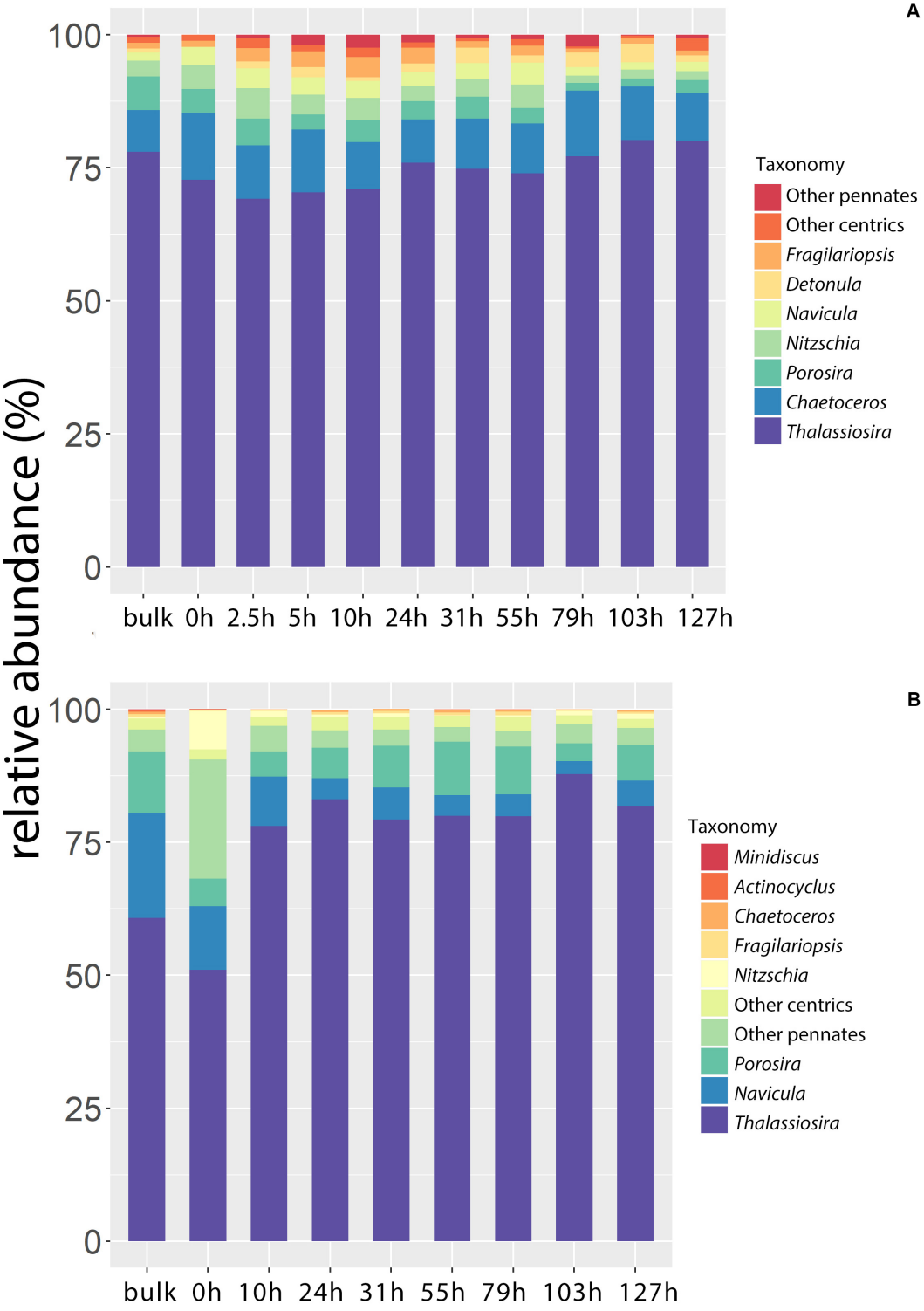

FIGURE 3 | The relative abundance of diatom genus or groups (%) in the bulk ice and during the incubation. **(A)** Light microscopy (LM); **(B)** 18S rDNA metabarcoding. The diatom genus or groups shown in the figure need to meet the following two standards: (1) The top 10 abundant ones (i.e., abundance of cells or gene fragments) during the whole incubation. (2) Genus or groups that were found at each time of sampling. Other genus or groups were added up to groups of other pennates and other centrics.

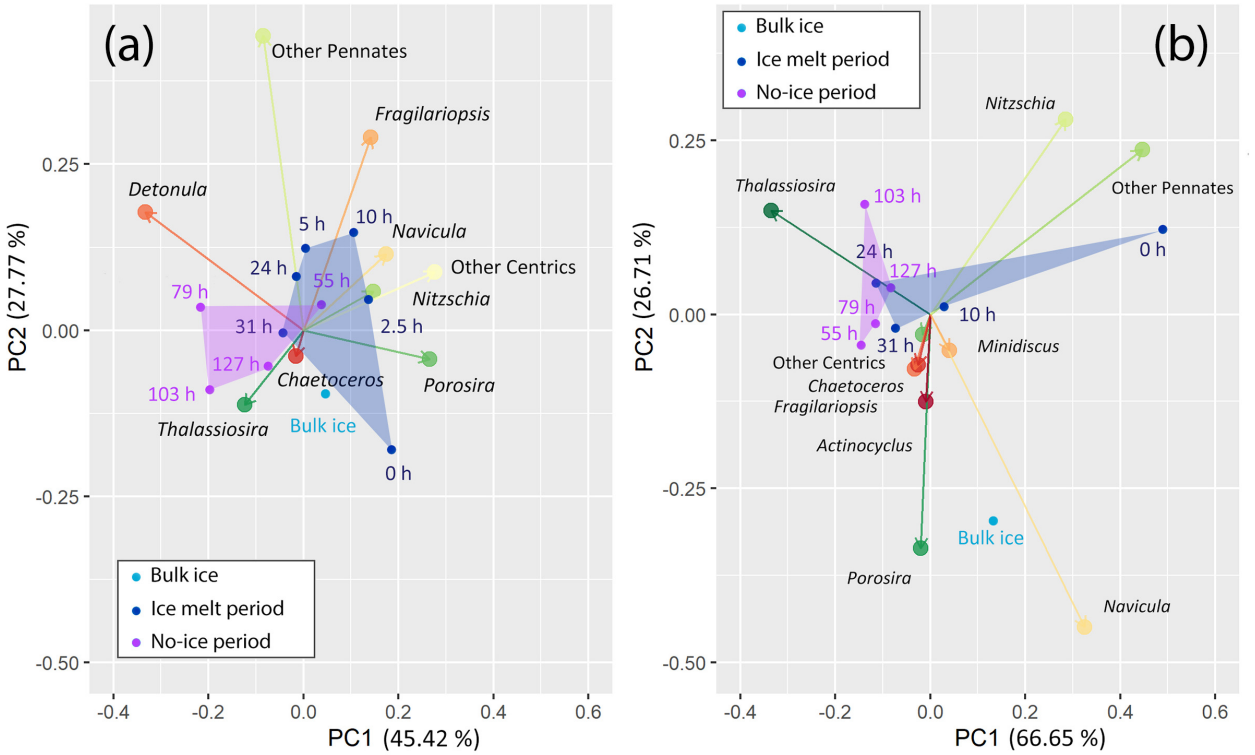

FIGURE 4 | Biplot of principal component analysis (PCA) on the community composition at different sampling times. **(a)** Light microscopy (LM); **(b)** 18S rDNA metabarcoding. Algal communities of different sampling times are in different colors: Light blue, bulk ice; navy, ice-melt period; purple, no-ice period. Algal communities of latter two sampling periods are in polygons. Hellinger distance is used for the ordination. The proportions shown in percent indicate the contributions of the principal components to the total variance in the community composition.

the western subarctic Pacific, including the Oyashio region and the northwestern Sea of Japan near Russia when the water temperatures were still <5°C (Ohwada, 1956; Sorokin and Sorokin, 1999; Motylkova and Konovalova, 2010; Suzuki et al., 2011; Yoshida et al., 2018). In particular, *T. nordenskioeldii* usually dominates the spring phytoplankton bloom in the shelf surface waters of the Sea of Okhotsk with water temperatures of 2–5°C and salinities of 20–27 (Sorokin and Sorokin, 1999). There is evidence that *Thalassiosira* is abundant in the eastern coastal waters of Sakhalin Island along the moving path of the drift ice in winter and after ice retreat (Sorokin and Sorokin, 1999; Leonov et al., 2007; Zakharkov et al., 2007). We thus suggest that *Thalassiosira* could be a common component in the drift ice of the Sea of Okhotsk and they play important roles in the drift ice and seawater in the Sea of Okhotsk during the winter and the ice melt season. Yoshida et al. (2018) reported that the spring phytoplankton communities of the shelf coastal Oyashio water differentiated from other Oyashio water masses by the presence and the dominance of *Thalassiosira*, suggesting a sea ice origin since the coastal Oyashio water is derived from sea ice meltwater within the Sea of Okhotsk (Ohtani, 1989). The pack ice even extends its influence to the Funka Bay of the southwestern Hokkaido that the seed populations of the *T. nordenskioeldii* bloom in spring was from the coastal Oyashio water and was transported southward by the lateral advection (Shinada et al., 1999). We thus suggest that the Okhotsk sea ice could be a source of those early spring blooms of *Thalassiosira* spp. in the coastal northwestern Pacific areas, indicating the seeding effect of the Okhotsk ice algae. And interestingly, we found a succession of *Thalassiosira* species during the no-ice period (**Supplementary Figure S3**). *T. nordenskioeldii* was the most abundant one in the bulk ice, while it was gradually outcompeted by *T. antarctica, T. hyalina* and *Thalassiosira* sp. In nature, *T. nordenskioeldii* is known to develop early in the growth season and disappears from the plankton community as the season advances along the northern coasts (Paasche, 1975). Zooplankton grazing might contribute to the succession in the field, while in this study it played a minor role because very few zooplankton were observed under the microscope. The mechanism of this succession is possibly related to the competition for nutrients and need to be studied in the future work.

Pennate diatoms had a larger abundance in the community of the bulk ice and at the beginning of the incubation (**Figures 3**, **4**). The decrease in the contribution during the later stage of the incubation was probably caused by the lower growth rate compared to that of the centric diatoms (**Figure 1**). The growth rate of pennate diatoms remained low in both the ice-melt and the no-ice periods. While the growth rate of centric diatoms increased by four-fold after complete ice melt. The community growth rate during the no-ice period, around 0.18 day^{-1}, was

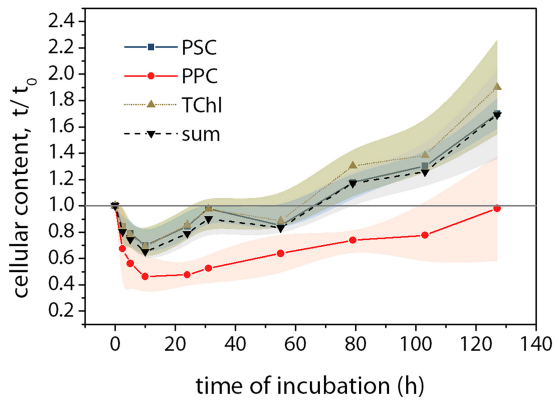

FIGURE 5 | Variations of pigment contents during the incubation compared to that at t_0. Pigments were analyzed using Ultra-High Performance Liquid Chromatography (UHPLC, Suzuki et al., 2015). Squares, photosynthetic carotenoids (PSC = fucoxanthin); Circles, photoprotective carotenoids (PPC = diadinoxanthin + diatoxanthin + β-carotene); upward triangles, total chlorophyll (TChl = Chl *c* + Chl *a*); downward triangles, the sum of all pigments. Mean values (±SD) are the average of four independent measurements.

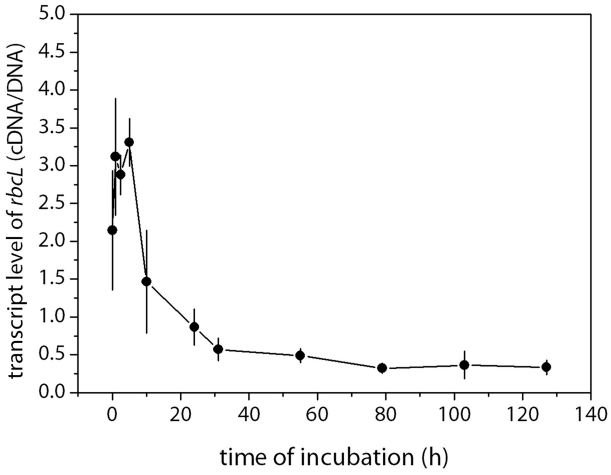

FIGURE 7 | Abundances of *rbcL* (cDNA) normalized to the gene copy number (cDNA/DNA) during the incubation. The transcription level of the genes was the cDNA gene copies standardized by the DNA gene copies in samples taken at the same time point. Mean values (±SD) are the average of four independent measurements.

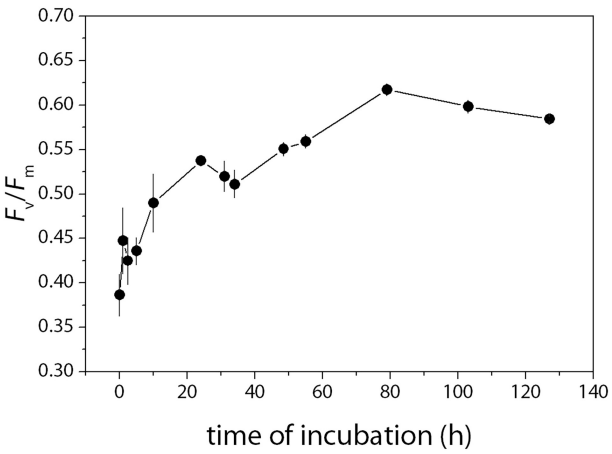

FIGURE 6 | Changes in the maximum photochemical efficiency of PSII (F_v/F_m) during the incubation. F_v/F_m was measured at each sampling time using a pulse amplitude modulated fluorometer (Water-PAM, Walz, Germany). The saturating pulse was provided by a red-LED with a peak illumination at 655 nm and set at 7,000 μmol photons m^{-2} s^{-1} and lasted for 400 ms for all measurements (Yan et al., 2019). The maximum photochemical efficiency of PSII was calculated as $F_v/F_m = (F_m - F_o)/F_m$. F_o is the minimum fluorescence after the darkness of 30 min and F_m is the maximum fluorescence under the saturation pulse. Mean values (±SD) are the average of four independent measurements.

mainly contributed by the centric diatoms and was slightly lower than the maximum growth rate of ice diatom isolates or communities under similar temperature, salinity and light conditions reported in previous studies (Gilstad and Sakshaug, 1990; Hegseth, 1992; Juhl and Krembs, 2010; Aslam et al., 2012, 2018; Olsen et al., 2017; Kulk et al., 2019). In those studies, the maximum growth rates of *T. antarctica*, *T. nordenskioeldii*, and *P. glacialis* under similar conditions were consistent and around 0.3 day^{-1} (Gilstad and Sakshaug, 1990; Kulk et al., 2019). While reported maximum growth rate for pennate diatoms were around 0.2 day^{-1} and was mainly collected from *Fragilariopsis cylindrus* and *Nitzschia frigida,* two representative pennate diatoms of the polar regions (Hegseth, 1992; Juhl and Krembs, 2010; Aslam et al., 2012, 2018). This indicates that pennate diatoms have the potential to grow while the intrinsic growth rate might be slower than centric diatoms under similar environmental conditions. We also suggest that the much slower growth rate of the pennate diatom of around 0.06 day^{-1} in this study could be partly due to the difference in the species composition of different communities investigated between our study and others. In our study, *Navicula* and *Nitzschia* were the most abundant pennate species in the bulk ice algal community (**Figures 3**, **4**), while the most well-investigated *F. cylindrus* by previous studies was seldom observed.

Navicula and *Nitzschia* usually occur in large abundance in the benthic algal communities (Chen et al., 2019). In the Sea of Okhotsk, sea ice is mainly formed on the northwestern shelf and off the eastern coast of Sakhalin Island (Martin et al., 1998). The sea ice is transported southward along the eastern coast of Sakhalin Island to the sampling area in the southern part of the sea (Ohshima et al., 2002). Ito et al. (2017) found the sediment materials were incorporated into sea ice during ice formation due to winter turbulent mixing in the northeast coast of Sakhalin Island. The seawater is affected by the water transported from the broad continental shelf in the northern Sea of Okhotsk (Ohshima et al., 2002). We thus suggest that some of the ice algal cells found in the drift ice, such as *Navicula* and *Nitzschia*, possibly come from those shallower coastal areas. There is evidence that growth of such pennate species that occur in both the benthic zone and sea ice could be inhibited under changing salinity

conditions. A study on the distribution and abundance of benthic epipelic diatoms along an estuarine gradient found that *Navicula* were more closely associated with the haline part of an estuary (Underwood et al., 1998). We thus suggest that such ice diatoms are possibly characterized by strong stenohalinity. In consistence with those findings, we found a larger percentage of dead cells in pennate diatoms during ice melt, suggesting that they were more susceptible to ice melting (**Figure 2**). In the field, ice melting contributed to the larger proportion of dead cells in surface waters of the Canadian Beaufort Sea during the Spring–Summer transition (Alou-Font et al., 2016). The results suggest that besides a lower intrinsic growth rate at a chilling temperature, the susceptibility to osmotic stress caused by ice melt is a more likely reason for the low growth rate of the pennate diatoms. On the other hand, the ecological success of *Thalassiosira* under stressful ice melt conditions could partly be attributed to their fast acclimation to salinity changes. In nature, *Thalassiosira* bloom is commonly observed in estuaries and coastal waters (Rijstenbil, 1987), suggesting their tolerance to mesohaline environments. Laboratory studies found some *Thalassiosira* species can tolerate salinities spanning 15–60 and had broad peaks spanning 25–45 for growth (Grant and Horner, 1976; Brand, 1984). Some species showed extreme euryhalinity and could even grew in freshwater medium (Brand, 1984). A summary of the effect of salinity on ice diatoms is shown in **Table 1**. In this study, the ice algal community dominated by *Thalassiosira* well-acclimated to the culture salinity from around 29 to 32.2. This is in agreement with previous studies that most ice algae can maintain normal photosynthesis and growth within the salinity range of 20 to 50. The data also suggest that pennate diatoms tend to be more sensitive to reduced salinities compared with centric diatoms.

The seeding of ice algae is dependent on the survival and sedimentation of algal cells (Haecky et al., 1998; Tedesco et al., 2012). Fast sinking results in a shorter residence time thus less contribution to the phytoplankton bloom (Haecky et al., 1998). Indeed, many pennate ice diatoms are characterized by rapid sedimentation during the ice melt season (Taguchi et al., 2000; Kauko et al., 2018; Selz et al., 2018). The sinking behavior of some pennate diatoms is first due to their preference for benthic habitats (Gradinger and Ikävalko, 1998). Additionally, there is evidence that diatom sinking is under direct metabolic control and is closely related to the cell size and energy availability, hence photosynthesis and respiration (Waite et al., 1992; Gemmell et al., 2016). High sinking rates are more often observed at low growth rates and in senescent cells when the energy becomes less sufficient (Smetacek, 1985; Waite et al., 1992; Durkin et al., 2016). Silicic acid limitation terminated the spring diatom bloom and triggered cell death, thus a fast sinking out of the photic layer in the Arctic near Greenland and Svalbard islands (Krause et al., 2019; Agustí et al., 2020). Our data suggests that the low energy availability and cell death due to inefficient photosynthesis under melt stress contributed to the fast sedimentation of some pennate ice diatoms, hence reducing their seeding effect to the open-water bloom.

The salt stress caused a 30% decrease in the cellular content of PSC and TChl after 10 h of incubation (**Figure 5**). We attribute this decrease to cell damage rather than acclimation due to the fact that abnormal cells were commonly observed at the beginning of the ice-melt period (**Supplementary Figure S2**). Similar cell deformation was also found in the large marine centric diatoms *Ditylum brightwellii* and *Corethron hystrix* when the cells were exposed to low salinities (Rijstenbil et al., 1989; Aizdaicher and Markina, 2010). For both species, lower salinity caused significant shrinkage of cytoplasm. Cytoplasm strands and chloroplasts moved to the center or edge of the cells in *D. brightwellii* (Rijstenbil et al., 1989). For *C. hystrix*, decreasing the medium salinity to 20 caused granular cellular contents and concentrated chloroplasts (Aizdaicher and Markina, 2010). Meanwhile, photosynthetic performance and cell division were severely inhibited (Rijstenbil et al., 1989). In our study, lower F_v/F_m at the beginning of the ice-melt indicated the malfunction of PSII (**Figure 6**). However, it appears that the functioning of photosynthesis of the investigated Okhotsk algal ice community was quite robust. Signs of F_v/F_m recovery have already appeared when sea ice was still in culture during the first day, and F_v/F_m showed a continuous increasing trend until day 4. It is worth noting that nearly half of the PPC pigments had been lost at t_{10} and the recovery progressed much slower than the other pigment groups. PPCs, especially diadinoxanthin (Ddx) and diatoxanthin (Dtx) are directly related to the non-photochemical quenching of chlorophyll fluorescence (NPQ) to dissipate excess excitation energy in diatoms through the diadinoxanthin-diatoxanthin cycle (the Ddx–Dtx Cycle) (Goss and Jakob, 2010; Lavaud and Lepetit, 2013). The Ddx–Dtx Cycle could be a common photoprotective strategy by ice diatoms to protect themselves against high light after being released to water columns (McMinn et al., 2010; Petrou et al., 2010, 2011; Reeves et al., 2011; Yan et al., 2019). The results of this study indicate that PPCs play a minor role in the acclimation to salinity fluctuations in the Okhotsk ice diatom communities.

We found sticky mucilage around diatom cells during the ice melt period (**Supplementary Figure S2**). The mucilage is referred to as extracellular polymeric substances (EPS) (Hoagland et al., 1993). Sea ice diatoms are known to produce polysaccharide-rich EPS (Krembs et al., 2002; Abdullahi et al., 2006). They function as cryoprotectants and osmoprotectants in sea ice by changing the physical structure of the ice pores to impede the desalination process while enhancing retention of organisms within the ice where light levels support substantial algal activity (Krembs et al., 2011). Under stressful conditions, the enhanced production of EPS is usually accompanied with increased transcript levels of genes related to carbon metabolism. Bussard et al. (2017) found an up-regulation of the genes related to carbon concentrating mechanisms (CCMs) in the model diatom *T. weissflogii* in response to lower salinities down to 20. Decreased temperature and increased salinity induced a significant up-regulation of the genes involved in carbohydrate metabolism of the ice diatom *F. cylindrus* in order to protect themselves from the stress caused by the freezing condition (Aslam et al., 2018). RubisCO catalyzes the first step of CO_2 fixation in photosynthesis. Due to the significant decrease in the turnover rate with temperature, high yield of this enzyme has been proposed as an adaptive mechanism under cold environments to the offset poor catalytic efficiency at low temperatures (Devos et al., 1998; Morgan-Kiss et al., 2006).

TABLE 1 | A summary of the effect of salinity on photosynthesis and growth of ice algae in previous studies.

Sampling site	Diatoms used	Culture temperature (°C)	Culture salinity	Salinity with almost no decrease in photosynthesis or growth	Salinity with no photosynthetic activity or growth	References
McMurdo Sound, Antarctica	Ice algal community dominated by *Nitzschia stellata*	−6, −2, and 6	0 to 100	30 to 50	100	Arrigo and Sullivan (1992)
Mertz Polynya, Antarctica	Ice algal community dominated by *Fragilariopsis curta*	2	10 to 30	28 to 30	None	Ryan et al. (2004)
Cape Hallett, Antarctica	Ice algal community dominated by *Nitzschia stellata* and *Fragilariopsis curta*	−0.7	16, 21, 35, 51 and 65	35 and 51	None	Ralph et al. (2007)
Gondwana Station in Terra Nova Bay, Antarctica	Ice algal community	−3	0, 12, 24 and 36	24 and 36	0	Ryan et al. (2011)
Isolates from Chukchi and Beaufort Seas in the vicinity of Barrow, Arctic	*Porosira glacialis, Thalassiosira bramaputrae*	5	5 to 70	10 to 50	5 and 70	Grant and Horner (1976)
	Melosira juergensii			15 to 35	5 and 70	
	Navicula transitans var. derasa			20 to 40	5, 15 and 70	
Laboratory work, isolates from the Greenland Sea, Arctic	*Nitzschia frigida*	−8 to −4	73, 109 and 145	73	None	Aletsee and Jahnke (1992)
	Thalassiosira antarctica			73	145	
Greenland Sea, Arctic	*Nitzschia arctica*	1	1 to 100	20.6 to 74	<12.2 and >90.8	Zhang et al. (1999)
	Chaetoceros spp.			4 to 74	>90.8	
	Pseudo-nitzschia pseudodelicatissima			4 to 56	>65.6	
Laboratory work	*Fragilariopsis nana* isolated from the Labrador Sea and *Fragilariopsis* sp. CCMP2297	3	5 to 150	5 to 33	150	Søgaard et al. (2011)

Indeed, we also found an eight-fold higher transcript levels of the *rbcL* gene during the ice melt period (**Figure 7**). The transcript levels under the ice melt condition was higher than that of the no-ice period for the samples taken at the similar time of the day ($p < 0.05$). This suggests that the cells made great efforts to do carbon fixation during the ice-melt period in need of protection and repairing.

CONCLUSION

The diatom *Thalassiosira* was a major component of the Okhotsk sea ice diatom community and has a great potential to seed the spring phytoplankton bloom not only in the Sea of Okhotsk, but also in coastal Oyashio waters of the western subarctic Pacific. The fast acclimation to salinity changes ensured the ecological success of *Thalassiosira*. Pennate diatoms of *Navicula* and *Nitzschia* were abundant in sea ice while their contribution decreased and became negligible as the incubation progressed. The growth of *Navicula* and *Nitzschia* was hindered by osmotic stress, indicated by higher mortality during the ice melt period. The inefficient photosynthesis and cell death under the melt stress significantly reduced the seeding potential of pennate ice diatoms.

DATA AVAILABILITY STATEMENT

The datasets presentede in this study can be found in online repositories. The names of the repository/repositories and accession number(s) can be found below: DDBJ under accession number PRJDB9641.

AUTHOR CONTRIBUTIONS

KS conceived this research. JN, TT, MI, and KS conducted the fieldwork. DY and KS designed the experiment. DY did the experiment and analyses. KY participated in the NGS part of the experiment. DY drafted the manuscript. DY, KY, JN, TT, and KS contributed to improving the final manuscript. All authors contributed to the article and approved the submitted version.

FUNDING

This work was partially supported by JSPS KAKENHI (Grant Numbers JP18H03352 and JP17H00775) and JSPS Research Fellowship for Young Scientists (Grant Number 20J10963).

ACKNOWLEDGMENTS

We thank the captain, crew and colleagues for supporting sea ice sampling during the P/V *Soya* SIRAS-19 expedition.

SUPPLEMENTARY MATERIAL

The Supplementary Material for this article can be found online at: https://www.frontiersin.org/articles/10.3389/fmars.2020.00613/full#supplementary-material

REFERENCES

Abdullahi, A. S., Underwood, G. J. C., and Gretz, M. R. (2006). Extracellular matrix assembly in diatoms (Bacillariophyceae). V. Environmental effects on polysaccharide synthesis in the model diatom, *Phaeodactylum tricornutum*. *J. Phycol.* 42, 363–378. doi: 10.1111/j.1529-8817.2006.00193.x

Agusti, S., González-Gordillo, J. I., Vaqué, D., Estrada, M., Cerezo, M. I., Salazar, G., et al. (2015). Ubiquitous healthy diatoms in the deep sea confirm deep carbon injection by the biological pump. *Nat. Commun.* 6:7608. doi: 10.1038/ncomms8608

Agustí, S., Krause, J. W., Marquez, I. A., Wassmann, P., Kristiansen, S., and Duarte, C. M. (2020). Arctic (Svalbard islands) active and exported diatom stocks and cell health status. *Biogeosciences* 17, 35–45. doi: 10.5194/bg-17-35-2020

Aizdaicher, N. A., and Markina, Z. V. (2010). The effect of decrease in salinity on the dynamics of abundance and the cell size of *Corethron Hystrix* (Bacillariophyta) in laboratory culture. *Ocean Sci. J.* 45, 1–5. doi: 10.1007/s12601-010-0001-8

Aletsee, L., and Jahnke, J. (1992). Growth and productivity of the psychrophilic marine diatoms *Thalassiosira antarctica* and *Nitzschia frigida* Grunow in batch cultures at temperatures below the freezing point of sea water. *Polar Biol.* 11, 643–647. doi: 10.1007/BF00237960

Alou-Font, E., Roy, S., Agustí, S., and Gosselin, M. (2016). Cell viability, pigments and photosynthetic performance of Arctic phytoplankton in contrasting ice-covered and open-water conditions during the spring-summer transition. *Mar. Ecol. Prog. Ser.* 543, 89–106. doi: 10.3354/meps11562

Arrigo, K. R., and Sullivan, C. W. (1992). The influence of salinity and temperature covariation on the photophysiological characteristics of Antarctic sea ice microalgae. *J. Phycol.* 28, 746–756. doi: 10.1111/j.0022-3646.1992.00746.x

Aslam, S. N., Cresswell−Maynard, T., Thomas, D. N., and Underwood, G. J. C. (2012). Production and characterization of the intra- and extracellular carbohydrates and polymeric substances (EPS) of three sea-ice diatom species, and evidence for a cryoprotective role for EPS. *J. Phycol.* 48, 1494–1509. doi: 10.1111/jpy.12004

Aslam, S. N., Strauss, J., Thomas, D. N., Mock, T., and Underwood, G. J. C. (2018). Identifying metabolic pathways for production of extracellular polymeric substances by the diatom *Fragilariopsis cylindrus* inhabiting sea ice. *ISME J.* 12:1237. doi: 10.1038/s41396-017-0039-z

Assur, A. (1960). *Composition of Sea Ice and Its Tensile Strength*. Wilmette, IL: U.S. Army Snow, Ice and Permafrost Research Establishment.

Baars, J. W. M. (1982). Autecological investigation on marine diatoms 3. Thalassiosira nordenskioeldii and Chaetoceros diadema. *Mar. Biol.* 68, 343–350. doi: 10.1007/BF00409599

Brand, L. E. (1984). The salinity tolerance of forty-six marine phytoplankton isolates. *Estuar. Coastal Shelf Sci.* 18, 543–556. doi: 10.1016/0272-7714(84)90089-1

Bussard, A., Corre, E., Hubas, C., Duvernois-Berthet, E., Corguillé, G. L., Jourdren, L., et al. (2017). Physiological adjustments and transcriptome reprogramming are involved in the acclimation to salinity gradients in diatoms. *Environ. Microbiol.* 19, 909–925. doi: 10.1111/1462-2920.13398

Chen, L., Weng, D., Du, C., Wang, J., and Cao, S. (2019). Contribution of frustules and mucilage trails to the mobility of diatom *Navicula* sp. *Sci. Rep.* 9, 1–12. doi: 10.1038/s41598-019-43663-z

Devos, N., Ingouff, M., Loppes, R., and Matagne, R. F. (1998). Rubisco adaptation to low temperatures: a comparative study in psychrophilic and mesophilic unicellular algae. *J. Phycol.* 34, 655–660. doi: 10.1046/j.1529-8817.1998.340655.x

Dixon, P. (2003). VEGAN, a package of R functions for community ecology. *J. Veget. Sci.* 14, 927–930. doi: 10.1111/j.1654-1103.2003.tb02228.x

Durkin, C. A., Mooy, B. A. S. V., Dyhrman, S. T., and Buesseler, K. O. (2016). Sinking phytoplankton associated with carbon flux in the Atlantic Ocean. *Limnol. Oceanogr.* 61, 1172–1187. doi: 10.1002/lno.10253

Endo, H., Ogata, H., and Suzuki, K. (2018). Contrasting biogeography and diversity patterns between diatoms and haptophytes in the central Pacific Ocean. *Sci. Rep.* 8, 1–13. doi: 10.1038/s41598-018-29039-9

Endo, H., Sugie, K., Yoshimura, T., and Suzuki, K. (2015). Effects of CO_2 and iron availability on *rbcL* gene expression in Bering Sea diatoms. *Biogeosciences* 12, 2247–2259. doi: 10.5194/bg-12-2247-2015

Endo, H., Yoshimura, T., Kataoka, T., and Suzuki, K. (2013). Effects of CO_2 and iron availability on phytoplankton and eubacterial community compositions in the northwest subarctic Pacific. *J. Exp. Mar. Biol. Ecol.* 439, 160–175. doi: 10.1016/j.jembe.2012.11.003

Ewert, M., and Deming, J. W. (2013). Sea ice microorganisms: environmental constraints and extracellular responses. *Biology (Basel)* 2, 603–628. doi: 10.3390/biology2020603

Fukamachi, Y., Shirasawa, K., Polomoshnov, A. M., Ohshima, K. I., Kalinin, E., Nihashi, S., et al. (2009). Direct observations of sea-ice thickness and brine rejection off Sakhalin in the Sea of Okhotsk. *Contin. Shelf Res.* 29, 1541–1548. doi: 10.1016/j.csr.2009.04.005

Garrison, D. L., Buck, K. R., and Fryxell, G. A. (1987). Algal assemblages in Antarctic pack ice and in ice-edge plankton. *J. Phycol.* 23, 564–572. doi: 10.1111/j.1529-8817.1987.tb04206.x

Garrison, D. L., and Close, A. R. (1993). Winter ecology of the sea ice biota in Weddell Sea pack ice. *Mar. Ecol. Prog. Ser.* 96, 17–31. doi: 10.3354/meps096017

Gemmell, B. J., Oh, G., Buskey, E. J., and Villareal, T. A. (2016). Dynamic sinking behaviour in marine phytoplankton: rapid changes in buoyancy may aid in nutrient uptake. *Proc. R. Soc. B Biol. Sci.* 283:20161126. doi: 10.1098/rspb.2016.1126

Gilstad, M., and Sakshaug, E. (1990). Growth rates of ten diatom species from the Barents Sea at different irradiances and day lengths. *Mar. Ecol. Prog. Ser.* 64, 169–173. doi: 10.3354/meps064169

Goss, R., and Jakob, T. (2010). Regulation and function of xanthophyll cycle-dependent photoprotection in algae. *Photosy. Res.* 106, 103–122. doi: 10.1007/s11120-010-9536-x

Gradinger, R., and Ikävalko, J. (1998). Organism incorporation into newly forming Arctic sea ice in the Greenland Sea. *J. Plankton Res.* 20, 871–886. doi: 10.1093/plankt/20.5.871

Granskog, M. A., Nomura, D., Müller, S., Krell, A., Toyota, T., and Hattori, H. (2015). Evidence for significant protein-like dissolved organic matter accumulation in Sea of Okhotsk sea ice. *Ann. Glaciol.* 56, 1–8. doi: 10.3189/2015AoG69A002

Grant, W. S., and Horner, R. A. (1976). Growth responses to salinity variation in four Arctic ice diatoms. *J. Phycol.* 12, 180–185. doi: 10.1111/j.1529-8817.1976.tb00498.x

Guillard, R. R. L., and Ryther, J. H. (1962). Studies of marine planktonic diatoms: I. *Cyclotella Nana* Hustedt, and *Detonula Confervacea* (cleve) Gran. *Can. J. Microbiol.* 8, 229–239. doi: 10.1139/m62-029

Haecky, P., Jonsson, S., and Andersson, A. (1998). Influence of sea ice on the composition of the spring phytoplankton bloom in the northern Baltic Sea. *Polar. Biol.* 20, 1–8. doi: 10.1007/s003000050270

Hegseth, E. N. (1992). Sub-ice algal assemblages of the Barents Sea: species composition, chemical composition, and growth rates. *Polar. Biol.* 12, 485–496. doi: 10.1007/BF00238187

Hernando, M., Schloss, I. R., Malanga, G., Almandoz, G. O., Ferreyra, G. A., Aguiar, M. B., et al. (2015). Effects of salinity changes on coastal Antarctic phytoplankton physiology and assemblage composition. *J. Exp. Mar. Biol. Ecol.* 466, 110–119. doi: 10.1016/j.jembe.2015.02.012

Hiwatari, T., Shirasawa, K., Fukamachi, Y., Nagata, R., Koizumi, T., Koshikawa, H., et al. (2008). Vertical material flux under seasonal sea ice in the Okhotsk Sea north of Hokkaido. Japan. *Polar Sci.* 2, 41–54. doi: 10.1016/j.polar.2008.02.003

Hoagland, K. D., Rosowski, J. R., Gretz, M. R., and Roemer, S. C. (1993). Diatom extracellular polymeric substances: function, fine structure, chemistry, and physiology. *J. Phycol.* 29, 537–566. doi: 10.1111/j.0022-3646.1993.00537.x

Horner (1985). *Sea Ice Biota*. Boca Raton, FL: CRC Press.

Ito, M., Ohshima, K. I., Fukamachi, Y., Mizuta, G., Kusumoto, Y., and Nishioka, J. (2017). Observations of frazil ice formation and upward sediment transport in the Sea of Okhotsk: a possible mechanism of iron supply to sea ice. *J. Geophys. Res. Oceans* 122, 788–802. doi: 10.1002/2016JC012198

Jahnke, J., and Baumann, M. (1983). Chemical and physical effects on the shape and growth of the diatom *Biddulphia sinensis* Greville in batch cultures: a contribution to bioindication in plankton ecology. *Hydrobiol. Bull.* 17, 5–20. doi: 10.1007/BF02255188

Japan Meteorological Agency (2020). *Sea ice in the Sea of Okhotsk*. Available online at: https://www.data.jma.go.jp/gmd/kaiyou/english/seaice_okhotsk/series_okhotsk_e.html (accessed April 17, 20200).

Juhl, A. R., and Krembs, C. (2010). Effects of snow removal and algal photoacclimation on growth and export of ice algae. *Polar Biol.* 33, 1057–1065. doi: 10.1007/s00300-010-0784-1

Kanna, N., Sibano, Y., Toyota, T., and Nishioka, J. (2018). Winter iron supply processes fueling spring phytoplankton growth in a sub-polar marginal sea, the Sea of Okhotsk: Importance of sea ice and the East Sakhalin Current. *Mar. Chem.* 206, 109–120. doi: 10.1016/j.marchem.2018.08.006

Kauko, H. M., Olsen, L. M., Duarte, P., Peeken, I., Granskog, M. A., Johnsen, G., et al. (2018). Algal colonization of young Arctic sea ice in spring. *Front. Mar. Sci.* 5:199. doi: 10.3389/fmars.2018.00199

Krause, J. W., Schulz, I. K., Rowe, K. A., Dobbins, W., Winding, M. H. S., Sejr, M. K., et al. (2019). Silicic acid limitation drives bloom termination and potential carbon sequestration in an Arctic bloom. *Sci. Rep.* 9:8149. doi: 10.1038/s41598-019-44587-4

Krell, A., Funck, D., Plettner, I., John, U., and Dieckmann, G. (2007). Regulation of proline metabolism under salt stress in the psychrophilic diatom *Fragilariopsis cylindrus* (bacillariophyceae). *J. Phycol.* 43, 753–762. doi: 10.1111/j.1529-8817.2007.00366.x

Krembs, C., Eicken, H., and Deming, J. W. (2011). Exopolymer alteration of physical properties of sea ice and implications for ice habitability and biogeochemistry in a warmer Arctic. *Proc. Natl. Acad. Sci. U.S.A.* 108, 3653–3658. doi: 10.1073/pnas.1100701108

Krembs, C., Eicken, H., Junge, K., and Deming, J. W. (2002). High concentrations of exopolymeric substances in Arctic winter sea ice: implications for the polar ocean carbon cycle and cryoprotection of diatoms. *Deep Sea Res. Part I* 49, 2163–2181. doi: 10.1016/S0967-0637(02)00122-X

Kudoh, S. (1993). Responses of microalgal primary productivity to the reduction of sea ice coverage in Lake Saroma during winter. *Bull. Plankton Soc. Jpn.* 39, 155–156.

Kulk, G., Buist, A., van de Poll, W. H., Rozema, P. D., and Buma, A. G. J. (2019). Size scaling of photophysiology and growth in four freshly isolated diatom species from Ryder Bay, western Antarctic peninsula. *J. Phycol.* 55, 314–328. doi: 10.1111/jpy.12813

Kuroda, H., Toya, Y., Watanabe, T., Nishioka, J., Hasegawa, D., Taniuchi, Y., et al. (2019). Influence of Coastal Oyashio water on massive spring diatom blooms in the Oyashio area of the North Pacific Ocean. *Prog. Oceanogr.* 175, 328–344. doi: 10.1016/j.pocean.2019.05.004

Lavaud, J., and Lepetit, B. (2013). An explanation for the inter-species variability of the photoprotective non-photochemical chlorophyll fluorescence quenching in diatoms. *Biochim. Biophys. Acta (BBA) Bioener.* 1827, 294–302. doi: 10.1016/j.bbabio.2012.11.012

Leonov, A. V., Mogil'nikova, T. A., Pishchal'nik, V. M., and Zenkin, O. V. (2007). Characteristic of microalgae development in the Sea of Okhotsk in winter and modeling of their annual dynamics in Aniva Bay. *Water Resour.* 34, 184–194. doi: 10.1134/S0097807807020091

Martin, S., Drucker, R., and Yamashita, K. (1998). The production of ice and dense shelf water in the Okhotsk Sea polynyas. *J. Geophys. Res.* 103, 27771–27782. doi: 10.1029/98JC02242

McMinn, A., Hattori, H., Hirawake, T., and Iwamoto, A. (2008). Preliminary investigation of Okhotsk Sea ice algae; taxonomic composition and photosynthetic activity. *Polar Biol.* 31, 1011–1015. doi: 10.1007/s00300-008-0433-0

McMinn, A., Martin, A., and Ryan, K. (2010). Phytoplankton and sea ice algal biomass and physiology during the transition between winter and spring (McMurdo Sound. Antarctica). *Polar Biol.* 33, 1547–1556. doi: 10.1007/s00300-010-0844-6

Michel, C., Legendre, L., and Taguchi, S. (1997). Coexistence of microalgal sedimentation and water column recycling in a seasonally ice-covered ecosystem (Saroma-ko Lagoon, Sea of Okhotsk, Japan). *J. Mar. Syst.* 11, 133–148. doi: 10.1016/S0924-7963(96)00034-6

Morgan-Kiss, R. M., Priscu, J. C., Pocock, T., Gudynaite-Savitch, L., and Huner, N. P. A. (2006). Adaptation and acclimation of photosynthetic microorganisms to permanently cold environments. *Microbiol. Mol. Biol. Rev.* 70, 222–252. doi: 10.1128/MMBR.70.1.222-252.2006

Motylkova, I. V., and Konovalova, N. V. (2010). Seasonal dynamics of phytoplankton in a lagoon-type lake Izmenchivoye (Southeast Sakhalin). *Russ. J. Mar. Biol.* 36, 86–92. doi: 10.1134/S1063074010020021

Mundy, C. J., Gosselin, M., Ehn, J. K., Belzile, C., Poulin, M., Alou, E., et al. (2011). Characteristics of two distinct high-light acclimated algal communities during advanced stages of sea ice melt. *Polar Biol.* 34, 1869–1886. doi: 10.1007/s00300-011-0998-x

Mustapha, M. A., and Saitoh, S.-I. (2008). Observations of sea ice interannual variations and spring bloom occurrences at the Japanese scallop farming area in the Okhotsk Sea using satellite imageries. *Estuar. Coast. Shelf Sci.* 77, 577–588. doi: 10.1016/j.ecss.2007.10.021

Notz, D., and Worster, M. G. (2009). Desalination processes of sea ice revisited. *J. Geophys. Res. Oceans* 114. doi: 10.1029/2008JC004885

Ohshima, K. I, Riser, S. C., and Wakatsuchi, M. (2005). Mixed layer evolution in the Sea of Okhotsk observed with profiling floats and its relation to sea ice formation. *Geophys. Res. Lett.* 32:L06607. doi: 10.1029/2004GL021823

Ohshima, K. I., Nihashi, S., Hashiya, E., and Watanabe, T. (2006). Interannual variability of sea ice area in the Sea of Okhotsk: Importance of surface heat flux in fall. *J. Meteorol. Soc. Jpn. Ser. II* 84, 907–919. doi: 10.2151/jmsj.84.907

Ohshima, K. I., Wakatsuchi, M., Fukamachi, Y., and Mizuta, G. (2002). Near-surface circulation and tidal currents of the Okhotsk Sea observed with satellite-tracked drifters. *J. Geophys. Res.* 107, 16–11. doi: 10.1029/2001JC001005

Ohtani, K. (1989). The role of the Sea of Okhotsk on the formation of the Oyashio Water. *Umi Sora* 65, 63–83.

Ohwada, M. (1956). Diatom communities in the Okhotsk Sea, principally on the west coast of Kamchatka, spring to summer 1955. *J. Oceanogr. Soc. Jpn.* 13, 29–34. doi: 10.5928/kaiyou1942.13.29

Okolodkov, Y. B. (1992). "Cryopelagic flora of the Chukchi, East Siberian and Laptev seas," in *Proceedings of the NIPR Symposium on Polar Biology*, Tokyo, 28–43.

Olsen, L. M., Laney, S. R., Duarte, P., Kauko, H. M., Fernández-Méndez, M., Mundy, C. J., et al. (2017). The seeding of ice algal blooms in Arctic pack ice: the multiyear ice seed repository hypothesis. *J. Geophys. Res. Biogeosci.* 122:2016JG003668. doi: 10.1002/2016JG003668

Paasche, E. (1975). Growth of the plankton diatom *Thalassiosira nordenskioeldii* Cleve at low silicate concentrations. *J. Exp. Mar. Biol. Ecol.* 18, 173–183. doi: 10.1016/0022-0981(75)90072-6

Petrou, K., Hill, R., Brown, C. M., Campbell, D. A., Doblin, M. A., and Ralph, P. J. (2010). Rapid photoprotection in sea-ice diatoms from the East Antarctic pack ice. *Limnol. Oceanogr.* 55, 1400–1407. doi: 10.4319/lo.2010.55.3.1400

Petrou, K., Hill, R., Doblin, M. A., McMinn, A., Johnson, R., Wright, S. W., et al. (2011). Photoprotection of sea-ice microalgal communities from the east Antarctic pack ice. *J. Phycol.* 47, 77–86. doi: 10.1111/j.1529-8817.2010.00944.x

Poulin, M., Daugbjerg, N., Gradinger, R., Ilyash, L., Ratkova, T., Quillfeldt, C., et al. (2011). The pan-Arctic biodiversity of marine pelagic and sea-ice unicellular eukaryotes: a first-attempt assessment. *Mar. Biodiv.* 41, 13–28. doi: 10.1007/s12526-010-0058-8

Qasim, S. Z., Bhattathiri, P. M. A., and Devassy, V. P. (1972). The influence of salinity on the rate of photosynthesis and abundance of some tropical phytoplankton. *Mar. Biol.* 12, 200–206. doi: 10.1007/BF00346767

Rajanahally, M. A., Sim, D., Ryan, K. G., and Convey, P. (2014). Can bottom ice algae tolerate irradiance and temperature changes? *J. Exp. Mar. Biol. Ecol.* 461, 516–527. doi: 10.1016/j.jembe.2014.10.005

Ralph, P. J., Ryan, K. G., Martin, A., and Fenton, G. (2007). Melting out of sea ice causes greater photosynthetic stress in algae than freezing in1. *J. Phycol.* 43, 948–956. doi: 10.1111/j.1529-8817.2007.00382.x

Reeves, S., McMinn, A., and Martin, A. (2011). The effect of prolonged darkness on the growth, recovery and survival of Antarctic sea ice diatoms. *Polar Biol.* 34, 1019–1032. doi: 10.1007/s00300-011-0961-x

Rijstenbil, J. W. (1987). Phytoplankton composition of stagnant and tidal ecosystems in relation to salinity, nutrients, light and turbulence. *Netherlands J. Sea Res.* 21, 113–123. doi: 10.1016/0077-7579(87)90027-5

Rijstenbil, J. W., Wijnholds, J. A., and Sinke, J. J. (1989). Implications of salinity fluctuation for growth and nitrogen metabolism of the marine diatom Ditylum brightwellii in comparison with *Skeletonema costatum*. *Mar. Biol.* 101, 131–141. doi: 10.1007/BF00393486

Roy, S., Llewellyn, C. A., Egeland, E. S., and Johnsen, G. (2011). *Phytoplankton Pigments: Characterization, Chemotaxonomy and Applications in Oceanography*. Cambridge: Cambridge University Press.

Różańska, M., Gosselin, M., Poulin, M., Wiktor, J. M., and Michel, C. (2009). Influence of environmental factors on the development of bottom ice protist communities during the winter–spring transition. *Mar. Ecol. Prog. Ser.* 386, 43–59. doi: 10.3354/meps08092

Ryan, K. G., Ralph, P., and McMinn, A. (2004). Acclimation of Antarctic bottom-ice algal communities to lowered salinities during melting. *Polar Biol.* 27, 679–686. doi: 10.1007/s00300-004-0636-y

Ryan, K. G., Tay, M. L., Martin, A., McMinn, A., and Davy, S. K. (2011). Chlorophyll fluorescence imaging analysis of the responses of Antarctic bottom-ice algae to light and salinity during melting. *J. Exp. Mar. Biol. Ecol.* 399, 156–161. doi: 10.1016/j.jembe.2011.01.006

Selz, V., Laney, S., Arnsten, A. E., Lewis, K. M., Lowry, K. E., Joy−Warren, H. L., et al. (2018). Ice algal communities in the Chukchi and Beaufort Seas in spring and early summer: composition, distribution, and coupling with phytoplankton assemblages. *Limnol. Oceanogr.* 63, 1109–1133. doi: 10.1002/lno.10757

Shcherbina, A. Y., Talley, L. D., and Rudnick, D. L. (2003). Direct observations of North Pacific ventilation: brine rejection in the Okhotsk Sea. *Science* 302, 1952–1955. doi: 10.1126/science.1088692

Shinada, A., Shiga, N., and Ban, S. (1999). Structure and magnitude of diatom spring bloom in Funka Bay, southwestern Hokkaido, Japan, as influenced by the intrusion of Coastal Oyashio Water. *Plankton Benthos Res.* 46, 22–29.

Shuntov, V. P. (2001). New data about seasonal distribution and migrations of whales and dolphins in the Sea of Okhotsk. *Russ. J. Mar. Biol.* 27, 201–208. doi: 10.1023/A:1011907218094

Smayda, T. J. (1969). Experimental observations on the influence of temperature, light, and salinity on cell division of the marine diatom, *Detonula confervacea* (Cleve) Gran. *J. Phycol.* 5, 150–157. doi: 10.1111/j.1529-8817.1969.tb02596.x

Smetacek, V. S. (1985). Role of sinking in diatom life-history cycles: ecological, evolutionary and geological significance. *Mar. Biol.* 84, 239–251. doi: 10.1007/BF00392493

Søgaard, D. H., Hansen, P. J., Rysgaard, S., and Glud, R. N. (2011). Growth limitation of three Arctic sea ice algal species: effects of salinity, pH, and inorganic carbon availability. *Polar Biol.* 34, 1157–1165. doi: 10.1007/s00300-011-0976-3

Sorokin, Y. I., and Sorokin, P. Y. (1999). Production in the Sea of Okhotsk. *J. Plankton Res.* 21, 201–230. doi: 10.1093/plankt/21.2.201

Suzuki, K., Kamimura, A., and Hooker, S. B. (2015). Rapid and highly sensitive analysis of chlorophylls and carotenoids from marine phytoplankton using ultra-high performance liquid chromatography (UHPLC) with the first derivative spectrum chromatogram (FDSC) technique. *Mar. Chem.* 176, 96–109. doi: 10.1016/j.marchem.2015.07.010

Suzuki, K., Kuwata, A., Yoshie, N., Shibata, A., Kawanobe, K., and Saito, H. (2011). Population dynamics of phytoplankton, heterotrophic bacteria, and viruses during the spring bloom in the western subarctic Pacific. *Deep Sea Res. Part 1 Oceanogr. Res. Pap.* 58, 575–589. doi: 10.1016/j.dsr.2011.03.003

Szymanski, A., and Gradinger, R. (2016). The diversity, abundance and fate of ice algae and phytoplankton in the Bering Sea. *Polar Biol.* 39, 309–325. doi: 10.1007/s00300-015-1783-z

Taguchi, S., Satoh, F., Hamaoka, S., Ikeda, M., Ishikawa, M., and Shirasawa, K. (2000). Effect of ice algal community on the increase of chlorophyll *a* concentration during spring in coastal water of the Sea of Okhotsk. *Polar Sci.* 13, 1–14.

Taguchi, S., Smith, R. E. H., and Shirasawa, K. (1997). Effect of silicate enrichment on ice algae at low salinity in Saroma-ko Lagoon, Hokkaido, Japan. *J. Mar. Syst.* 11, 45–52. doi: 10.1016/S0924-7963(96)00026-7

Talley, L. D., and Nagata, Y. (1995). The Okhotsk Sea and Oyashio Region. Sidney, British Columbia: North Pacific Marine Science Organization (PICES). Available online at: http://aquaticcommons.org/1331/ (accessed January 30, 2020).

Tedesco, L., Vichi, M., and Scoccimarro, E. (2019). Sea-ice algal phenology in a warmer Arctic. *Sci. Adv.* 5:eaav4830. doi: 10.1126/sciadv.aav4830

Tedesco, L., Vichi, M., and Thomas, D. N. (2012). Process studies on the ecological coupling between sea ice algae and phytoplankton. *Ecol. Model.* 226, 120–138. doi: 10.1016/j.ecolmodel.2011.11.011

Tomas, C. R. (1997). *Identifying Marine Phytoplankton*. Amsterdam: Elsevier.

Toyota, T., Takatsuji, S., Tateyama, K., Naoki, K., and Ohshima, K. I. (2007). Properties of sea ice and overlying snow in the Southern Sea of Okhotsk. *J. Oceanogr.* 63, 393–411. doi: 10.1007/s10872-007-0037-2

Underwood, G. J. C., Phillips, J., and Saunders, K. (1998). Distribution of estuarine benthic diatom species along salinity and nutrient gradients. *Eur. J. Phycol.* 33, 173–183. doi: 10.1080/09670269810001736673

Waite, A. M., Thompson, P. A., and Harrison, P. J. (1992). Does energy control the sinking rates of marine diatoms? *Limnol. Oceanogr.* 37, 468–477. doi: 10.4319/lo.1992.37.3.0468

Yan, D., Endo, H., and Suzuki, K. (2019). Increased temperature benefits growth and photosynthetic performance of the sea ice diatom *Nitzschia* cf. *neglecta* (Bacillariophyceae) isolated from Saroma Lagoon, Hokkaido, Japan. *J. Phycol.* 55, 700–713. doi: 10.1111/jpy.12846

Yoshida, K., Endo, H., Lawrenz, E., Isada, T., Hooker, S. B., Prášil, O., et al. (2018). Community composition and photophysiology of phytoplankton assemblages in coastal Oyashio waters of the western North Pacific during early spring. *Estuar. Coast. Shelf Sci.* 212, 80–94. doi: 10.1016/j.ecss.2018.06.018

Yoshida, K., Seger, A., Kennedy, F., McMinn, A., and Suzuki, K. (2020). Freezing, melting and light stress on the photophysiology of ice algae: *ex situ* incubation of the ice algal diatom *Fragilariopsis cylindrus* (Bacillariophyceae) using an ice tank. *J. Phycol.* (in press). doi: 10.1111/jpy.13036

Zakharkov, S. P., Selina, M. S., Vanin, N. S., Shtraikhert, E. A., and Biebov, N. (2007). Phytoplankton characteristics and hydrological conditions in the western part of the Sea of Okhotsk in the spring of 1999 and 2000 based on expeditionary and satellite data. *Oceanology* 47, 519–530. doi: 10.1134/S0001437007040091

Zhang, C. I., Radchenko, V., Sugimoto, T., and Hyun, S. M. (2006). *Interdisciplinary physical and biological processes of the Sea of Okhotsk and the Japan/East Sea: The Global Coastal Ocean: Interdisciplinary Regional Studies and Syntheses, Pan-regional syntheses and the Coasts of North and South America and Asia (Harvard University Press)*. Available online at: https://www.researchgate.net/publication/233823630_Interdisciplinary_physical_and_biological_processes_of_the_Sea_of_Okhotsk_and_the_JapanEast_Sea_11S (accessed January 21, 2020).

Zhang, Q., Gradinger, R., and Spindler, M. (1999). Experimental study on the effect of salinity on growth rates of Arctic-sea-ice algae from the Greenland Sea. *Bor. Environ. Res.* 99, 1–8.

Conflict of Interest: The authors declare that the research was conducted in the absence of any commercial or financial relationships that could be construed as a potential conflict of interest.